

# Isolation, Expansion, and Endoscopic Delivery of Autologous Enteric Neuronal Stem Cells in Swine

Cell Transplantation  
Volume 32: 1–12  
© The Author(s) 2023  
Article reuse guidelines:  
sagepub.com/journals-permissions  
DOI: 10.1177/09636897231215233  
journals.sagepub.com/home/cll



Ryo Hotta<sup>1</sup> , Weikang Pan<sup>1</sup>, Sukhada Bhawe<sup>1</sup>, Nandor Nagy<sup>2</sup>, Rhian Stavely<sup>1</sup>, Takahiro Ohkura<sup>1</sup>, Kumar Krishnan<sup>3</sup>, Geoffrey de Couto<sup>4</sup>, Richard Myers<sup>4</sup>, Luis Rodriguez-Borlado<sup>4</sup>, Alan J. Burns<sup>4,5</sup>, and Allan M. Goldstein<sup>1</sup>

## Abstract

The enteric nervous system (ENS) is an extensive network of neurons and glia within the wall of the gastrointestinal (GI) tract that regulates many essential GI functions. Consequently, disorders of the ENS due to developmental defects, inflammation, infection, or age-associated neurodegeneration lead to serious neurointestinal diseases. Despite the prevalence and severity of these diseases, effective treatments are lacking as they fail to directly address the underlying pathology. Neuronal stem cell therapy represents a promising approach to treating diseases of the ENS by replacing the absent or injured neurons, and an autologous source of stem cells would be optimal by obviating the need for immunosuppression. We utilized the swine model to address key questions concerning cell isolation, delivery, engraftment, and fate in a large animal relevant to human therapy. We successfully isolated neural stem cells from a segment of small intestine resected from 1-month-old swine. Enteric neuronal stem cells (ENSCs) were expanded as neurospheres that grew optimally in low-oxygen (5%) culture conditions. Enteric neuronal stem cells were labeled by lentiviral green fluorescent protein (GFP) transduction, then transplanted into the same swine from which they had been harvested. Endoscopic ultrasound was then utilized to deliver the ENSCs (10,000–30,000 neurospheres per animal) into the rectal wall. At 10 and 28 days following injection, autologously derived ENSCs were found to have engrafted within rectal wall, with neuroglial differentiation and no evidence of ectopic spreading. These findings strongly support the feasibility of autologous cell isolation and delivery using a clinically useful and minimally invasive technique, bringing us closer to first-in-human ENSC therapy for neurointestinal diseases.

## Keywords

cell therapy, enteric neuropathies, autologous, swine, endoscopic ultrasound

## Introduction

Enteric neuropathies result from congenital or acquired abnormalities of the enteric nervous system (ENS) and include conditions, such as congenital aganglionosis (Hirschsprung's disease; HSCR), esophageal achalasia, chronic intestinal pseudo-obstruction, and gastroparesis. Despite the prevalence and severity of these diseases, current medical and surgical approaches aim to relieve the symptoms of the disease instead of directly addressing the underlying pathophysiology. Cell therapy offers the potential to treat the underlying pathophysiology by replacing the missing or damaged ENS by transplanting neural progenitors to restore the ENS and improve gut function. A number of studies have demonstrated successful isolation, expansion, and transplantation

<sup>1</sup> Department of Pediatric Surgery, Massachusetts General Hospital, Boston, MA, USA

<sup>2</sup> Department of Anatomy, Histology and Embryology, Faculty of Medicine, Semmelweis University, Budapest, Hungary

<sup>3</sup> Division of Gastroenterology, Department of Internal Medicine, Massachusetts General Hospital, Boston, MA, USA

<sup>4</sup> Gastrointestinal Drug Discovery Unit, Takeda Development Center Americas, Inc., Cambridge, MA, USA

<sup>5</sup> Stem Cells and Regenerative Medicine, UCL Great Ormond Street Institute of Child Health, London, UK

Submitted: June 24, 2023. Revised: September 22, 2023. Accepted: November 1, 2023.

### Corresponding Author:

Allan M. Goldstein, Department of Pediatric Surgery, Massachusetts General Hospital, 55 Fruit Street, Warren 1153, Boston, MA, USA.  
Email: amgoldstein@partners.org



**Table 1.** Primary Antibodies Used in This Study.

Antibody (clone)	Host	Dilution	Source of antibody, catalog number	Figure
Anna-1 (Hu)	Human IgG	1:16,000	Kindly gifted by Lennon lab	Fig. 1D–I
$\alpha$ SMA	Rabbit IgG	1:200	Abcam (ab5694)	Figs. 1D, E, 2B&E
Calretinin	Rabbit	1:100	Invitrogen	Fig. 1G
GFAP	Rabbit IgG	1:400	DAKO/Agilent	Fig. 2H
GFP	Goat IgG	1:400	Rockland	Fig. 5D–G
HuC/HuD	Mouse IgG2a	1:100	Invitrogen (A-21271)	Fig. 2D
NCAM	Rabbit IgG	1:200	Invitrogen (PA5-78402)	Fig. 2G
PGP9.5	Rabbit IgG	1:100	Abcam (ab27053)	Fig. 1C, J
P75	Rabbit IgG	1:400	Promega (G3231)	Figs. 2F, 5F
Sox10	Mouse IgG1	1:50	Santa Cruz Biotechnology (sc-365692)	Fig. 2J
S100	Rabbit IgG	1:100	Thermo Fisher Scientific	Figs. 1I, 5G
S100	Rabbit	1:100	Neomarkers	Fig. 2M
Tuj1	Mouse IgG1	1:300	Novus Biologicals (NB600-1018)	Fig. 2L, M
Tuj1 (conj)	Mouse IgG2a	1:100	Biolegend	Figs. 2K, 5E
Tuj1	Mouse IgG2a	1:200	Covance (MMS-435P)	Fig. 2I

$\alpha$ SMA: alpha-smooth muscle actin; GFAP: glial fibrillary acidic protein; GFP: green fluorescent protein; NCAM: neural cell adhesion molecule.

of enteric neuronal stem cells (ENSCs) to animal models of enteric neuropathies<sup>1–4</sup> with functional recovery<sup>5,6</sup> and even improved survival in mice with HSCR<sup>7,8</sup>. These promising findings support the feasibility of cell-based therapy for enteric neuropathies. However, several issues have to be taken into consideration for its future clinical application.

Optimization of cell delivery methods is critically important. Favorable features include a minimally invasive approach and the ability to target accurately the appropriate layer of the gut wall. Endoscopic cell delivery under ultrasound guidance can accomplish this. Endoscopy is commonly used for the diagnosis and treatment of gastrointestinal (GI) diseases. We and others have reported successful and efficient delivery of cells to the gut wall using colonoscopy in mice<sup>9–11</sup>, but utilization of endoscopic ultrasound (EUS) to improve targeting within the gut wall has not been previously reported. Endoscopic ultrasound is commonly used to perform preoperative staging of GI tumors<sup>12,13</sup> based on its ability to allow visualization of the layers of the intestinal wall, leading us to propose EUS for targeting ENSC delivery to the muscularis propria of rectum.

To test the feasibility of this approach, we used the porcine model because of the size equivalency to human infants as an initial proof-of-concept for eventual application of this technique for delivery of ENSCs to infants with HSCR, in which the rectosigmoid colon is missing enteric ganglia. Furthermore, the experimental model we established allows us to harvest a segment of small intestine from the same swine thus permits testing of the feasibility of autologous cell transplantation. Since immunological and ethical difficulties are challenging hurdles for the use of other cell sources, autologously derived ENSCs are advantageous for clinical application. In this study, we demonstrate the successful isolation, expansion, and labeling of autologous swine ENSCs, with successful transplantation via EUS-guided fine-needle injection to the

rectal wall, where engraftment and neuronal differentiation without ectopic spreading were achieved.

## Methods

### Animals

All animal protocols were approved by the Institutional Animal Care and Use Committee at Massachusetts General Hospital (MGH; Protocol #2018N000027). Female Yorkshire swine (age, 4–6 weeks; body weight, ~15 kg) were purchased from Tufts Comparative Medicine Services (Tufts University, MA) and housed in the animal facility at MGH.

### Tissue Preparation and Immunohistochemistry

Tissue preparation and immunohistochemistry were performed as previously described<sup>14</sup>. Cells, preparation of longitudinal muscle and myenteric plexus (LMMP), and full-thickness gut samples were fixed in 4% paraformaldehyde. For cryosections, full-thickness samples were embedded in 15% sucrose at 4°C overnight, and then in 15% sucrose plus 7.5% gelatin at 37°C for 1 h. The tissue was rapidly frozen at –50°C in nitrogen. Frozen sections were collected on glass slides at 12–14  $\mu$ m thickness with a Leica CM3050 S cryostat (Leica, Buffalo Grove, IL). For immunohistochemical staining, samples were permeabilized with 0.1% Triton X-100 and blocked with 10% donkey serum for 30 min. Primary antibodies (Table 1) were diluted in 2% donkey serum, 0.01% Triton X-100, and incubated with tissues at 4°C overnight. For wholemount staining of swine LMMP, 10% donkey serum or bovine serum albumin (BSA) in phosphate-buffered saline Tween-20 (PBST; 0.1% Triton X-100 in phosphate-buffered saline [PBS]) was used for blocking, primary antibodies were incubated for 3 days on a

shaker at 4°C, followed by addition of secondary antibodies for 2 days.

Secondary antibodies included the following: donkey anti-rabbit IgG (1:500; Alexa Fluor 488 and 546; Thermo Fisher Scientific, Waltham, MA), donkey anti-goat IgG (1:500; Alexa Fluor 488; Thermo Fisher Scientific), goat anti-mouse IgG (1:500; Alexa Fluor 488; Thermo Fisher Scientific), and donkey anti-human IgG (1:200, Alexa Fluor 488 and 647; Thermo Fisher Scientific). Cell nuclei were identified with 4',6-diamidino-2-phenylindole (DAPI) solution (Vector Labs, Burlingame, CA) and sections were mounted with aqua-poly/mount (Fisher Scientific). Images were taken using a Nikon A1R laser scanning confocal microscope (Nikon Instruments, Melville, NY) or a KeyenceBZX-700All-In-OneMicroscopy (Keyence, IL).

### *Harvest Intestinal Tissue From Swine*

Animals were fasted from the night before the operation. Anesthesia induction and maintenance was with isoflurane after endotracheal intubation. Carprofen (Rimadyl, 2 mg/kg), buprenorphine (Buprenex, 0.01 mg/kg), and cefazolin 40 mg/kg were administered intramuscularly (IM) prior to the operation. A laparotomy was created via a 5 cm vertical midline incision was made below the umbilicus. A segment (5–10 cm) of small bowel was resected following ligation of mesenteric vessels. The resected specimen was brought to the laboratory for cell harvesting. End-to-end bowel anastomosis was performed using two layers of interrupted 4-0 Vicryl sutures. The abdominal wall was closed in two layers with 0 polydioxanone suture (PDS) and the skin closed with staples. Local analgesia was given intradermally using 10 ml of 0.5% bupivacaine (Marcaine). Fentanyl patch (25 mcg/h) was applied and kept in place for 72 hours postoperatively. Animals were recovered from anesthesia at the animal facility under careful monitoring. Regular diet was commenced on post-operative Day 1.

### *Tissue Processing, Cell Isolation, and Culture*

Intestinal tissues were kept in Hanks' balanced salt solution (HBSS, Thermo Fisher Scientific) on ice during transfer. Tissue dissection and dissociation commenced within 1 h after the animal had been euthanized. Small intestine was used for cell isolation. Muscularis propria, including the longitudinal muscle, circular muscle, and myenteric plexus, was separated from the underlying submucosa using forceps. Tissues were enzymatically dissociated with 0.75 mg/ml Liberase Thermolysin High formulation (Roche, Indianapolis, IN) and DNase 1 (1 mg/ml, Sigma Aldrich, St Louis, MO) at 37°C without mincing. Overnight (up to 18 h) digestion was typically required for full tissue dissociation. Pellets were obtained and washed with prewarmed complete medium, followed by resuspension in Dulbecco's modified Eagle medium: nutrient

mixture F-12 (DMEM/F12, Gibco, Life Technologies) supplemented with 1:100 glutamax (Gibco), 1:100 N<sub>2</sub> (STEMCELL Technologies, Vancouver, BC), 1:50 B27 without vitamin A (Fisher Scientific), 20 ng/ml basic fibroblast growth factor (bFGF; STEMCELL Technologies), 20 ng/ml EGF (Fisher Scientific), 1:1,000 beta-mercaptoethanol (Sigma Aldrich), 1:1,000 heparin (STEMCELL Technologies), 1:500 primocin (Fisher Scientific), and 50 µg/ml metrodinazole (Sigma Aldrich). Cells were counted and plated at a density of 100,000 live cells/ml of complete media in T75 flasks and cultured to form enteric neurospheres for 10–14 days. A 1:1 media change was performed every 3 days.

### *Viral Production and Transduction*

Lentivirus vector expressing fluc (firefly luciferase) and green fluorescent protein (GFP), separated by an internal ribosomal entry site, under the control of the cytomegalovirus (CMV) promoter<sup>15</sup> with a titer of  $2.3 \times 10^8$ – $1.0 \times 10^9$  IU/ml was prepared by the MGH Viral Vector Core Facility (MGH Neuroscience Center, Charlestown, MA). Enteric neurospheres formed as above were gently triturated to single cell suspensions using Accutase (STEMCELL Technologies). Lentivirus was added at multiplicity of infection (MOI) in the range of 5–100. After 48 h, successful transduction was confirmed by GFP expression. To determine transduction efficiency, enteric neurospheres were generated from lentiviral transduced ENSCs, dissociated and plated on fibronectin-coated cover slips, and the presence of GFP fluorescence quantitatively measured using ImageJ software.

### *EUS-Guided Injection of Autologously Derived Swine ENSCs to the Rectum*

Recipient swine were anesthetized as above and fecal material removed from the rectum digitally and with irrigation. A suspension of neurospheres was prepared (10,000–30,000 neurospheres in 0.5–1.0 ml saline containing 1:100 India ink). Endoscopy was performed to visualize the rectal lumen followed by (GF-UCT180, Olympus America, PA, USA) guided cell injection through a 22G endoscopic needle. For preliminary experiments, three different injection materials with different colors (Table 2) were used to optimize targeting of the injection site.

## **Results**

Small intestinal resection was performed on 4- to 6-week-old female Yorkshire swine and the tissue processed for immunohistochemistry to characterize the ENS and identify antibodies that can be used in this species (Table 1). Staining with the neuronal marker, PGP9.5, shows nerve fibers projecting to the intestinal villi (Fig. 1C, arrows). Hu+ neuronal cell bodies (Fig. 1D, arrows) and P75+ glial cells (Fig. 1F)



**Table 2.** Injection Materials.

Product	Vendor	Color	Notes, references
FluoSpheres™	Thermo Fisher	Fluorescent red (580/605)	Polystyrene microspheres, 15 μm in diameter
Fluorescent microspheres	Cospheric	GFP	Polystyrene microspheres, 53–63 μm in diameter
Tissue dyes	Davidson Marking System	Yellow	Chitnis et al <sup>16</sup>

GFP: green fluorescent protein.

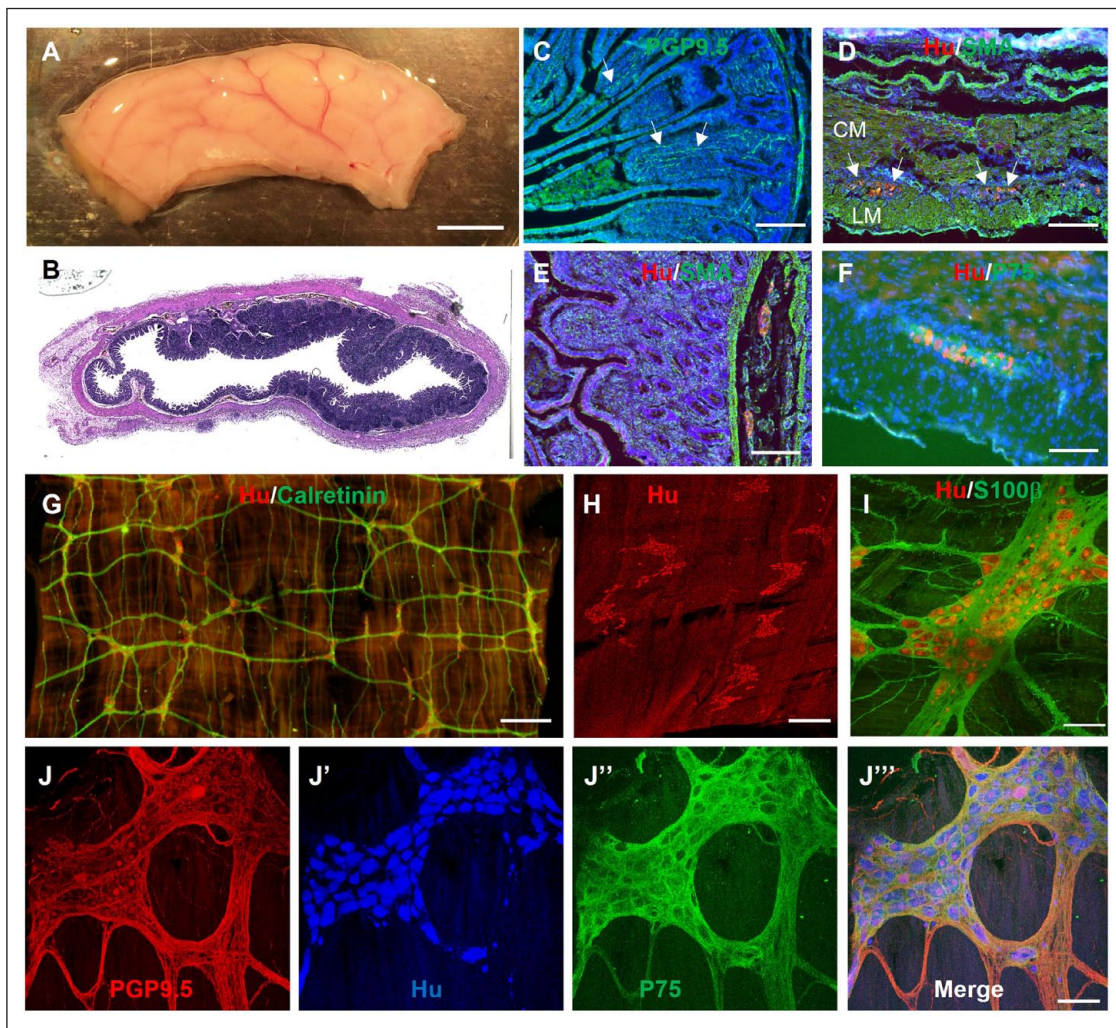


**Figure 1.** Immunofluorescent characterization of swine small intestine ENS. (A) Segment of swine small intestine was harvested and processed for H&E (B) and immunohistochemistry, including PGP9.5 (C), Hu/SMA (D, E), and Hu/P75 (F). Wholemount immunostaining of the myenteric plexus with Hu and calretinin reveals the myenteric ganglia with interconnecting nerve fibers (G). High-power images of myenteric ganglia show enteric neurons (PGP9.5, Hu) and glia (S100β, P75) (I, J–J’’’). Scale bars: A, 1 cm; G, 1 mm; H, 500 μm; E, 200 μm; C, D, F, I, and J, 100 μm. CM: circular muscle; ENS: enteric nervous system; GFP: green fluorescent protein; LM: longitudinal muscle; SMA: smooth muscle actin.

are present in the myenteric ganglia located between the SMA+ circular and longitudinal muscle layers (Fig. 1D). Submucosal enteric ganglia are also visualized with Hu (Fig. 1E). Wholemount preparations of the muscularis propria from 4- to 6-week-old swine small intestine were also stained immunohistochemically (Fig. 1G–J). Enteric ganglia with

interconnecting fibers label with the neuronal markers Hu and calretinin (Fig. 1G). High-power image reveals Hu+ neurons surrounded by S100β+ glia in a myenteric ganglion (Fig. 1H, I). The interconnected myenteric neuroglial network is visualized with PGP9.5 staining of neuronal fibers, Hu+ neuronal cell bodies, and P75+ enteric glia (Fig. 1J)

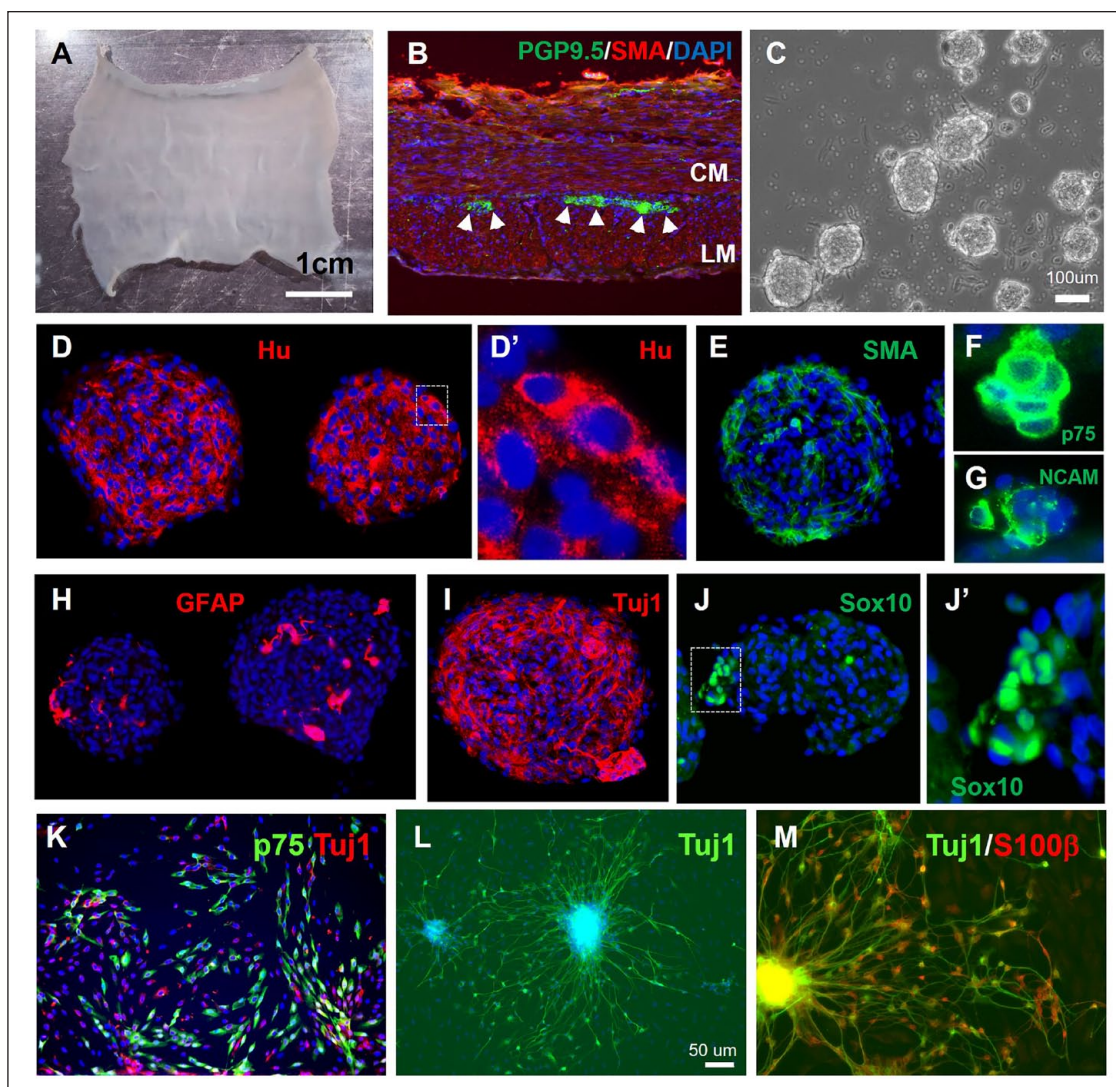


**Figure 2.** Isolation, characterization, and differentiation of swine ENSCs. (A) Small intestinal muscularis propria was isolated by microdissection. (B) Cross-sections show PGP9.5+ myenteric neurons between the SMA-expressing circular muscle (CM) and longitudinal muscle (LM). Following tissue digestion and culture for 10 days, enteric neurospheres are formed (C). Immunohistochemical characterization confirms presence of neurons expressing Hu (D, D'), smooth muscle (E); and glial cells expressing P75 (F), NCAM (G), GFAP (H), Tuj1 (I), and Sox10 (J, J'). After neurosphere dissociation, cells were cultured on a fibronectin-coated surface, where Tuj1+ neurons (K, L) and P75+/S100B+ (K, M) glia are seen. Scale bars: A, 1 cm; C, 100  $\mu$ m; L, 50  $\mu$ m. ENSC: enteric neuronal stem cell; GFP: green fluorescent protein; SMA: smooth muscle actin.

To isolate swine ENSCs, the muscularis propria was mechanically separated from a segment of small intestine (Fig. 2A,  $n = 16$ ). Immunofluorescence of a cross-section confirms the presence of myenteric ganglia between the two muscle layers (Fig. 2B, arrowheads). Following mechanical and enzymatic dissociation, cells were plated and cultured for 10–14 days to form enteric neurospheres (Fig. 2C). Immunohistochemical characterization of the neurospheres showed they contain neurons that label with Hu (Fig. 2D–D'), NCAM (Fig. 2G), and Tuj1 (Fig. 2I), SMA-expressing smooth muscle cells (Fig. 2E), and markers that label both enteric glia and neuronal progenitors, including P75 (Fig. 2F), GFAP

(Fig. 2H), and Sox10 (Fig. 2J–J'). To determine the differentiation potential of swine ENSCs, neurospheres were dissociated and cultured on fibronectin-coated coverslips for 7 days. Cells extend fiber projections and express markers of neurons (Tuj1,  $33.9 \pm 14.1\%$  of all DAPI+ cells,  $n = 3$ ) and glia (P75, S100B,  $34.9 \pm 11.2\%$  of all DAPI+ cells,  $n = 3$ ) (Fig. 2K–M).

To develop ENSCs as a potential regenerative cell therapy, we first aimed to identify potential growth conditions to maximize cell numbers and the proportion of neuronal progenitors. Compounds tested included a 5HT4 agonist (RS67506), N2 supplement (commonly used for neural stem



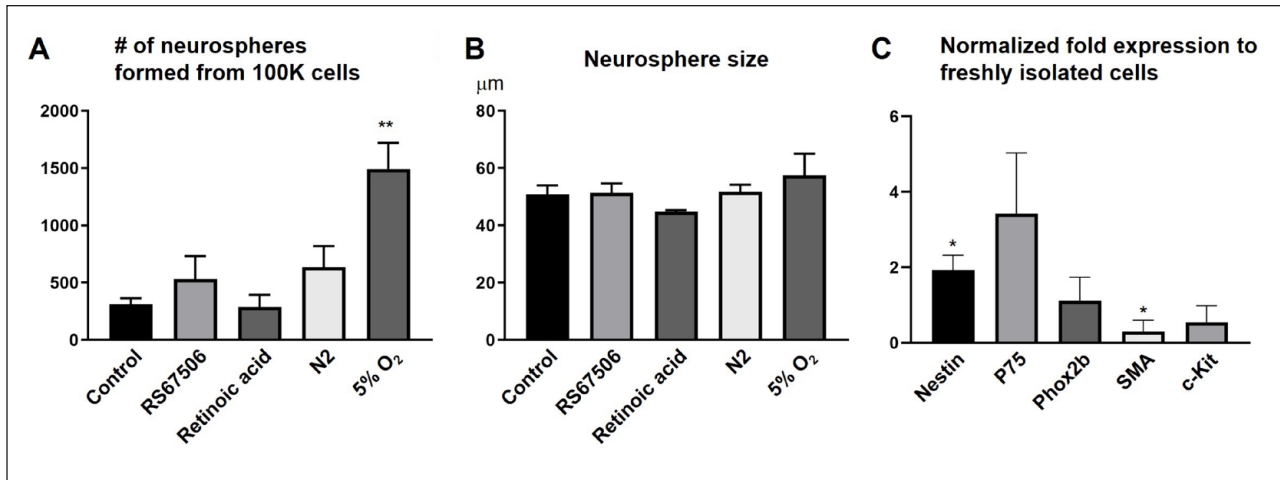


**Figure 3.** Optimizing culture conditions for swine ENSCs. (A) ENSCs cultured in 5% O<sub>2</sub> conditions formed significantly more enteric neurospheres than those grown in control conditions (20% O<sub>2</sub>) or in the presence of various other putative growth factors. No change was observed in neurosphere size (B). Neurospheres grown in 5% O<sub>2</sub> exhibit significantly increased levels of Nestin transcript and decreased expression of SMA, relative to transcript levels in freshly isolated cells (C, \* $P < 0.05$ ). RS67506: 5HT<sub>4</sub> agonist. ENSC: enteric neuronal stem cell; SMA: smooth muscle actin.

cell expansion), and retinoic acid, but these did not lead to an improvement in the number of neurospheres generated (Fig. 3A). In contrast, culturing neurospheres in 5% oxygen dramatically enhanced the number of neurospheres (Fig. 3A,  $313.3 \pm 50.5$  in Control vs  $1492.5 \pm 242.3$  in 5% O<sub>2</sub>, \*\*  $p < 0.01$ ). No change was observed in their size (Fig. 3B). qPCR was performed on RNA extracted from the neurospheres to determine whether low-oxygen conditions altered gene expression as an indicator of whether growth in these conditions expanded particular cell types. Gene expression in the neurospheres was compared to that in primary ENSCs just after harvesting and prior to culture. Results show a two-fold increase in the expression of Nestin and a significantly lower expression of SMA in neurospheres (Fig. 3C), suggesting that growth in hypoxia conditions supports expansion of the neural stem cell population while also potentially inhibiting the growth of myofibroblasts.

We developed a protocol for isolation and transplantation of autologous ENSCs to the swine rectum, as shown in Fig. 4A ( $n = 6$ ). A segment of small intestine was resected from 4–6-week-old Yorkshire swine via laparotomy with the animal under general anesthesia (Fig. 4A, Day 0). End-to-end anastomosis was performed with 4-0 Vicryl sutures. Harvested bowel was brought to the laboratory and processed for neurosphere formation as described above. After 10–14 days in culture, enteric neurospheres formed. To allow identification of ENSCs following transplant, cells were labeled by transduction with a lentiviral vector expressing GFP. This was done by dissociating the neurospheres to a single cell suspension and then adding viral particles at an MOI ranging from 5 to 100. After 48 hours, successful viral transduction was confirmed by GFP expression (Fig. 4B). Transduction efficiency was quantified by counting GFP+

cells as a proportion of all cells following neurosphere dissociation and plating on fibronectin-coated cover slips. There was a dose-dependent increase observed, with  $62.0 \pm 6.0\%$  transduction efficiency at an MOI of 100 (Fig. 4C).

Lenti-GFP transduction was performed on dissociated cells after 14 days of neurosphere culture, and the cells allowed to re-form neurospheres over an additional 7 days (Fig. 4A). On Day 21, swine were transplanted with their own autologously derived GFP+ ENSCs using EUS to target the cells to the appropriate layer of the rectal wall. Animals were anesthetized and placed in the lateral position. Fecal material was removed manually and by irrigation from the anorectum. Endoscopic ultrasound (GF-UCT180, Olympus America, PA, USA) was used to visualize the layers of the rectal wall (Fig. 4D). A single injection of 0.5–1.0 ml cell suspension (containing 10–30,000 neurospheres) was performed using a 22G endoscopic needle advanced through the scope (Fig. 4E). Animals also were injected with  $1.0 \times 10^6$  red fluorescent protein (RFP) beads, India ink, as well as yellow and green dye to determine the accuracy of targeting specific layers and to facilitate later identification of the cell injection site. At 10 days ( $n = 2$ ) after transplantation, animals were euthanized and the anorectum harvested to determine the success of cell delivery, survival, and differentiation *in vivo*. As shown in Fig. 5, the areas stained with green dye (green arrows), yellow dye (yellow arrows), and India ink (Fig. 5A, white arrows) are easily identified. The site where GFP+ ENSCs and RFP beads were injected (dashed circle) was examined by microscopy (Fig. 5B, dotted circle). After cryosection and H&E staining of the recipient rectum, we observed successful targeting of various layers of the GI tract: yellow dye spread along the submucosa and green dye was present in deeper layers and

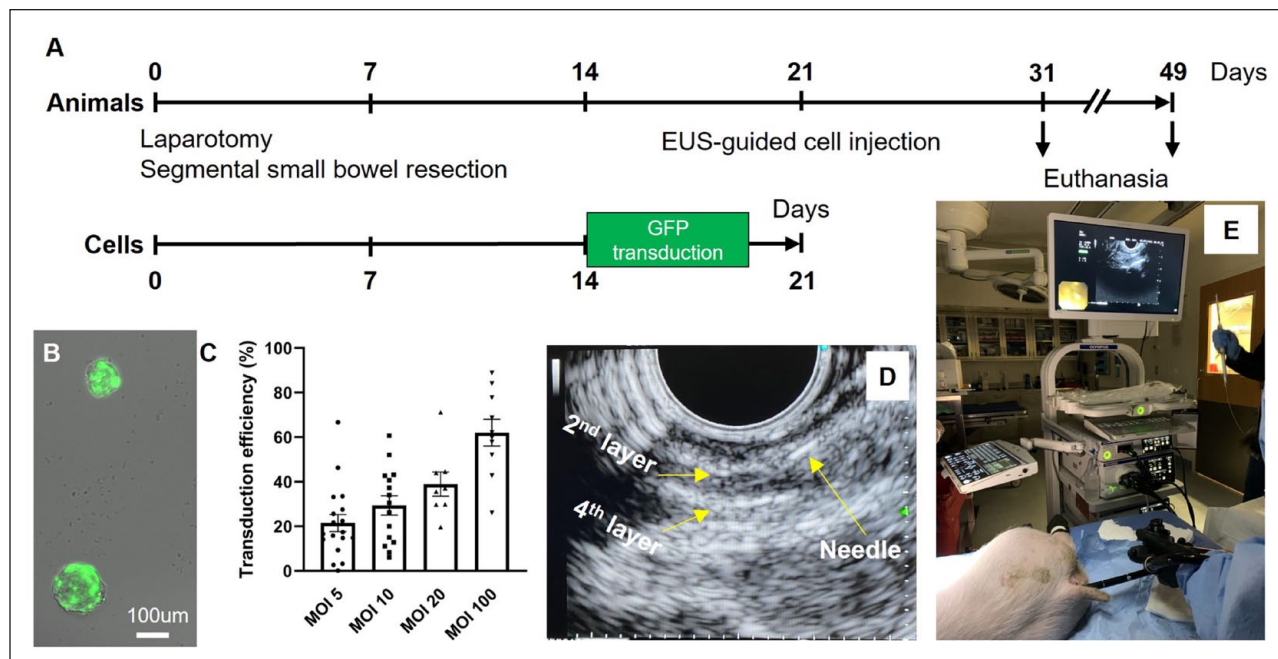


**Figure 4.** Isolation, expansion, and labeling of autologous ENSCs followed by *in vivo* transplantation to swine rectum. (A) Overview of the experimental design. (B) Representative image shows neurospheres transduced with a lentiviral-GFP vector following determination of the optimal multiplicity of infection (MOI, C). Endoscopic ultrasound (EUS) was used to visualize the layers of the rectal wall (D, second and fourth layer represent the submucosal and serosal layer, respectively) to target colonoscopic injection of the ENSC suspension (E). ENSC: enteric neuronal stem cell.

within the circular muscular (Fig. 5C). Immunohistochemical staining shows RFP beads (Fig. 5D, white arrows) and GFP+ ENSCs within the rectal submucosal layer (Fig. 5D, green arrows).

Sections of transplanted rectum were immunostained with neuronal and glial markers to assess ENSC differentiation following transplantation. A subpopulation of GFP+ ENSCs were immunoreactive for Tuj1 (Fig. 5E, G, and H, arrows), suggesting neuronal differentiation. Immunostaining for S100 $\beta$  confirmed that GFP+ transplanted ENSCs cells underwent glial differentiation (Fig. 5F). To determine whether any ectopic distribution of ENSCs to remote sites occurred, several recipient animals ( $n = 3$ ) were maintained for 4 weeks after cell transplantation and the following tissues were sampled following euthanasia: mesenteric lymph nodes, liver, lung, and spleen. PCR was performed with GFP-specific primers to detect the presence of transplanted cells in those tissue. No GFP was detected, suggesting that transplanted ENSCs did not migrate outside of the gut.

## Discussion

In this study, we utilized a large animal model to test the feasibility of isolating, expanding, and delivering autologously derived ENSCs for the treatment of enteric neuropathies. Importantly, we found that culturing swine ENSCs in reduced oxygen conditions led to a marked increase in the

number and purity of ENSCs. Following successful labeling of ENSCs using lentiviral GFP vector, we were able to deliver autologous ENSCs to the rectal wall using EUS. This allowed accurate targeting of the gut layer with successful engraftment and differentiation of autologous ENSCs. No remote ectopic cell spread was observed at 4 weeks following injection. These observations are highly supportive of the potential for utilizing autologous cells for the treatment of neurointestinal diseases.

The porcine gut has been increasingly proposed as a useful model for human translational studies because of its many similarities to human intestine<sup>17,18</sup>. The swine ENS has been characterized extensively and shares commonalities with the human ENS, including architecture and chemical coding<sup>19–22</sup>, physiological properties<sup>23,24</sup> and transcriptomic signatures<sup>25</sup>. There are known anatomical differences between pig and human colon, such as the spiral orientation and absence of an appendix in the former<sup>17</sup>. However, the size and anatomy of the anorectal region in neonatal pigs is almost identical to that of human infants, and their small intestines are long enough to tolerate segmental small bowel resection<sup>26</sup> for harvesting autologous ENSCs. We therefore chose the swine as the best translational model for us to test the feasibility of autologous ENSCs isolation and transplantation.

Cell therapy offers the potential to replace the ENS in patients with neurointestinal disorders. We and others have demonstrated successful isolation and expansion of neural

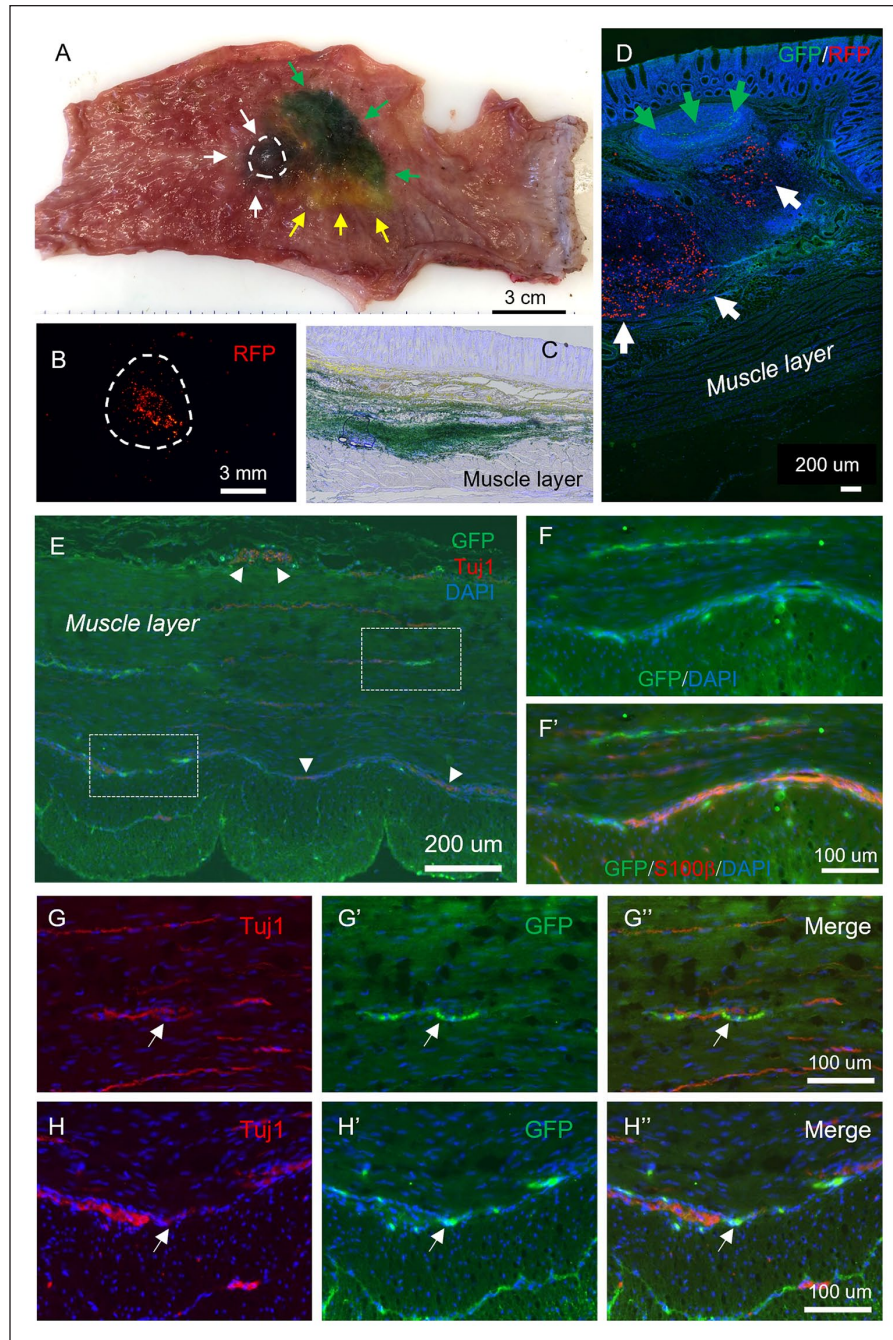


**Figure 5.** Identification of transplanted ENSCs and their differentiation within the rectum. (A) Rectum was explanted immediately following EUS-guided colonoscopic injection of multiple colored dyes into the rectal wall: green dye (green arrows), yellow dye (yellow arrows), and black ink (white arrows and circle). High-power imaging identified the injected RFP beads (B). Sections of recipient gut reveal successful targeting of the submucosa and muscularis layers with dye (C), and identification of GFP<sup>+</sup> cells (D, green arrows) and RFP beads (D, white arrows) within the submucosal layer. Immunohistochemistry shows transplanted GFP<sup>+</sup> ENSCs give rise to neurons (TuJ1; E, G, and H, arrows; arrowheads indicate endogenous plexus) and glial cells (F, S100 $\beta$ ). High-power images of white dotted boxes in E are shown in (G and H). ENSC: enteric neuronal stem cell; EUS: endoscopic ultrasound; RFP: red fluorescent protein.

progenitors from embryonic and postnatal rodents<sup>27–30</sup>, and from patients with neurointestinal disorders<sup>5,31,32</sup>. These cells have been shown to possess the ability to engraft, migrate, and differentiate into functioning neurons, with restoration of gut function *in vivo*<sup>2,3,6,28</sup>. Although these observations

strongly support the potential of ENSCs for treating neurointestinal disorders, previous studies<sup>7,33</sup> required immunosuppression for transplant recipients. Since the toxicities associated with long-term use of immunosuppression are well known<sup>34,35</sup>, it would be extremely advantageous to avoid



the need for these medications. Autologous gut-derived cells are therefore an optimal cell source for regenerative therapy since they avoid immunologic concerns, as well as the practical, ethical, and tumorigenic concerns raised by other cell sources, such as central nervous system-derived, fetal-derived, or induced pluripotent stem cells (iPSCs)-derived neural stem cells<sup>36</sup>.

To date, three potential autologous sources of neural progenitors have been described in the field of neurogastroenterology. Rollo et al<sup>37</sup> isolated ENSCs from human colonic tissues surgically resected from patients with HSCR. Following their expansion in culture in the presence of GSK3 inhibitor, those human autologous ENSCs were transplanted into explants of aganglionic colonic muscle from the same patient from whom the ENSCs had been harvested<sup>37</sup> and showed successful engraftment and neuroglial differentiation *ex vivo*. This was the first study demonstrating the feasibility of using autologous ENSCs for treating HSCR. Subsequently, Fattahi et al<sup>7</sup> generated enteric neural progenitors (ENPs) from pluripotent stem cells, another potential autologous cell source for regenerative medicine. Enteric neural progenitors derived from human pluripotent stem cells (PSCs) were transplanted into the colon of mouse models of HSCR, revealing extensive migratory ability with differentiation into appropriate phenotypes, including enteric neuron subtypes, and ultimately restoring colonic motility and improving their survival<sup>7,8</sup>. These milestone studies added great value to the potential of cell-based approaches for the treatment of neurointestinal diseases, but use of human cells raised immunological difficulties, requiring use of *ex vivo* colonic muscle explants<sup>37</sup> or immunocompromised recipient animals<sup>7,8</sup>. More recently, another source of neural progenitors has been established from skin: skin-derived precursors (SKPs)<sup>38</sup>. Thomas et al obtained 1.2–1.7 million SKPs from each cm<sup>2</sup> of abdominal or shoulder skin of minipigs and injected these to aganglionic colon created by serosal application of benzalkonium chloride, a detergent used to generate experimental aganglionosis. Successful engraftment and neuroglial differentiation of SKPs was seen at 7 days post-transplantation<sup>38</sup>, but they exhibited limited capacity of proliferation and differentiation<sup>38</sup> and it has not yet been shown whether SKPs can produce neuromuscular connectivity with GI smooth muscle. In the current study, we focused on isolating neural progenitors from a segment of small intestine, which can be easily harvested from the patient, thereby providing a convenient autologous cell source. We successfully maximized cell yield by culturing them in reduced oxygen condition, which has been described previously for ENSCs isolated from mice. However, we observed a more than four-fold increase in the number of cells obtained from swine bowel tissue. Ten- to 14-day culture in reduced oxygen also supported the preferential growth of neural progenitors, as shown by our quantitative polymerase chain reaction (qPCR) analysis. These findings are critically important for establishing research and clinical

protocols to utilize ENSCs in the future and provide strong support for the feasibility of using autologous cells for treating enteric neuropathies.

Endoscopic ultrasound-guided injection offers a safe, efficient, and minimally invasive approach to deliver cells to the wall of the GI tract. Several studies including ours have shown that endoscopy allows effective delivery of cancer cells<sup>10</sup> or neural progenitors<sup>9</sup> to the wall of murine colon. It is well known in developmental biology that environmental cues provided by the gut mesenchyme are important for progenitor cells to differentiate into appropriate phenotypes and acquire normal function<sup>39–41</sup>. Therefore, placing ENSCs in the right layer can be important to maximize the effect of cell transplantation to treat neurointestinal diseases. Endoscopic ultrasound has evolved from a purely diagnostic imaging modality to an interventional procedure that provides a minimally invasive alternative to interventional radiologic and surgical techniques<sup>42</sup>. Endoscopic ultrasound-guided fine-needle aspiration has been established as a tissue acquisition method<sup>43,44</sup>, for drainage, ablation, or even necrosectomy in pancreatic and hepatobiliary disease<sup>45–48</sup>, and for vascular access<sup>49,50</sup>, celiac plexus block<sup>51,52</sup>, or injection of antitumoral agents<sup>53,54</sup>. In the current study, EUS successfully visualized the layers of the swine rectum and allowed effective cell delivery. Although histological examination of recipient colon revealed their successful engraftment and neuroglial differentiation of, it is unknown how important the appropriate location is and even which layer is optimal. In fact, previous reports have demonstrated that neural progenitors injected to intraperitoneal cavity can home to the gut wall, engraft, and differentiate into neurons within the wall of the gut *in vivo*<sup>55,56</sup>. Moreover, we and others have observed neural progenitor cells can migrate across the muscle layers or penetrate through serosa and extend fibers toward the endogenous myenteric plexus and intestinal mucosa<sup>28,57,58</sup>. Therefore, it may not be necessary to deliver the cells to the intermyenteric layer for them to survive and elicit function. Further studies to compare the efficiency of cell engraftment within the different layers of GI tract are required.

This work has several limitations. As a proof-of-concept study demonstrating the feasibility of harvesting and transplanting autologous ENSCs into the rectal wall in a large animal model, we did not assess the function of the cells following transplantation or their contributions to colonic motility. To date, only a few reports have described a porcine model of colonic aganglionosis created by focal ablation of the ENS using topical application of benzalkonium chloride to the serosa of rectosigmoid colon<sup>38,59</sup>. Although none of the studies include functional characterization of aganglionic porcine colon, this model can be useful to determine if the aganglionic gut environment is permissive for transplanted autologous ENSCs in a large animal setting. We recently observed that the area grafted by ENSCs correlates with the degree of functional improvement in colonic motility in a mouse model of enteric neuropathy. Endoscopic cell delivery

would allow multiple injections of cells to maximize the cell coverage over the recipient colon. Future studies will be warranted to determine how efficiently multiple cell injections can optimize cell coverage in the colorectum of large animals and whether this correlates with colonic motor function.

### Acknowledgements

The authors thank Dr Vanda Lennon (Mayo Clinic) for providing human anti-Anna-1 (Hu) antibody. The lentiviral GFP virus was prepared at the MGH Vector Core Facility, Massachusetts General Hospital Neuroscience Center. The authors wish to acknowledge the support and expertise of the Knight Surgical Research Core staff in support of this research.

### Authors' Contributions

Conceptualization, R.H., R.M., L.R.B., A.J.B., and A.M.G.; methodology, R.H., W.P., S.B., T.O., and K.K.; formal analysis, S.B., W.P., R.S., N.N., and T.O.; investigation, R.H., S.B., W.P., and R.S.; resources, R.M., A.J.B., and A.M.G.; data curation, R.H., W.P., R.S., S.B., N.N., and O.T.; writing original draft preparation, R.H. and S.B.; writing review and editing, G.C., L.R.B., R.M., A.J.B., and A.M.G.; visualization, R.H., S.B., W.P., R.S., and T.O.; supervision, R.M., L.R.B., A.J.B., and A.M.G.; funding acquisition, A.M.G. All authors have read and agreed to the published version of the manuscript.

### Availability of Data and Materials

All data are available upon request to the corresponding author.

### Ethical Approval

This study was approved by our institutional review board.

### Statement of Human and Animal Rights

This article does not contain any studies with human or animal subjects.

### Statement of Informed Consent

There are no human subjects in this article and informed consent is not applicable.

### Research Ethics

This study was reviewed and approved by the Institutional Animal Care and Use Committee at Massachusetts General Hospital (Protocol #2018N000027, "Enteric neuronal cell therapy for neuro-intestinal disease," approved on 4/27/2021).

### Declaration of Conflicting Interests

The author(s) declared the following potential conflicts of interest with respect to the research, authorship, and/or publication of this article: G.C., L.R.B., R.M., and A.J.B. are employees of Takeda Development Center Americas and hold stock and/or stock options in Takeda. R.H., W.P., S.B., N.N., R.S., T.O., K.K., and A.M.G. do not possess any competing interest.

### Funding

The author(s) disclosed receipt of the following financial support for the research, authorship, and/or publication of this article: This research was funded by Takeda Development Center Americas.

### ORCID iD

Ryo Hotta  <https://orcid.org/0000-0001-9890-8241>

### References

- Hotta R, Cheng LS, Graham HK, Nagy N, Belkind-Gerson J, Mattheolabakis G, Amiji MM, Goldstein AM. Delivery of enteric neural progenitors with 5-HT4 agonist-loaded nanoparticles and thermosensitive hydrogel enhances cell proliferation and differentiation following transplantation in vivo. *Biomaterials*. 2016;88:1–11.
- Cooper JE, McCann CJ, Natarajan D, Choudhury S, Boesmans W, Delalande JM, Vanden Berghe P, Burns AJ, Thapar N. In vivo transplantation of enteric neural crest cells into mouse gut; engraftment, functional integration and long-term safety. *PLoS One*. 2016;11(1):e0147989.
- Stamp LA, Gwynne RM, Foong JP, Lomax AE, Hao MM, Kaplan DI, Reid CA, Petrou S, Allen AM, Bornstein JC, Young HM. Optogenetic demonstration of functional innervation of mouse colon by neurons derived from transplanted neural cells. *Gastroenterology*. 2017;152:1407–18.
- Hetz S, Acikgoez A, Voss U, Nieber K, Holland H, Hegewald C, Till H, Metzger R, Metzger M. In vivo transplantation of neurosphere-like bodies derived from the human postnatal and adult enteric nervous system: a pilot study. *PLoS One*. 2014;9(4):e93605.
- Lindley RM, Hawcutt DB, Connell MG, Almond SN, Vannucchi MG, Faussone-Pellegrini MS, Edgar DH, Kenny SE. Human and mouse enteric nervous system neurosphere transplants regulate the function of aganglionic embryonic distal colon. *Gastroenterology*. 2008;135(1):205–16.
- McCann CJ, Cooper JE, Natarajan D, Jevans B, Burnett LE, Burns AJ, Thapar N. Transplantation of enteric nervous system stem cells rescues nitric oxide synthase deficient mouse colon. *Nat Commun*. 2017;8:15937.
- Fattahi F, Steinbeck JA, Kriks S, Tchieu J, Zimmer B, Kishinevsky S, Zeltner N, Mica Y, El-Nachef W, Zhao H, de Stanchina E, et al. Deriving human ENS lineages for cell therapy and drug discovery in Hirschsprung disease. *Nature*. 2016;531(7592):105–9.
- Fan Y, Hackland J, Baggiolini A, Hung LY, Zhao H, Zumbo P, Oberst P, Minotti AP, Hergenreder E, Najjar S, Huang Z, et al. hPSC-derived sacral neural crest enables rescue in a severe model of Hirschsprung's disease. *Cell Stem Cell*. 2023;30(3):264–82.e9.
- Cheng LS, Hotta R, Graham HK, Nagy N, Goldstein AM, Belkind-Gerson J. Endoscopic delivery of enteric neural stem cells to treat Hirschsprung disease. *Neurogastroenterol Motil*. 2015;27(10):1509–14.
- Zigmond E, Halpern Z, Elinav E, Brazowski E, Jung S, Varol C. Utilization of murine colonoscopy for orthotopic implantation of colorectal cancer. *PLoS One*. 2011;6(12):e28858.
- Beyaz S, Mana MD, Roper J, Kedrin D, Saadatpour A, Hong SJ, Bauer-Rowe KE, Xifaras ME, Akkad A, Arias E, Pinello

- L, et al. High-fat diet enhances stemness and tumorigenicity of intestinal progenitors. *Nature*. 2016;531(7592):53–8.
12. Malmstrom ML, Saftoiu A, Vilmann P, Klausen TW, Gogenur I. Endoscopic ultrasound for staging of colonic cancer proximal to the rectum: a systematic review and meta-analysis. *Endosc Ultrasound*. 2016;5(5):307–14.
  13. Mocellin S, Pasquali S. Diagnostic accuracy of endoscopic ultrasonography (EUS) for the preoperative locoregional staging of primary gastric cancer. *Cochrane Database Syst Rev*. 2015;2015(2):CD009944.
  14. Pan W, Rahman AA, Stavely R, Bhave S, Guyer R, Omer M, Picard N, Goldstein AM, Hotta R. Schwann cells in the aganglionic colon of Hirschsprung disease can generate neurons for regenerative therapy. *Stem Cells Transl Med*. 2022;11:1232–44.
  15. Teng J, da Hora CC, Kantar RS, Nakano I, Wakimoto H, Batchelor TT, Chiocca EA, Badr CE, Tannous BA. Dissecting inherent intratumor heterogeneity in patient-derived glioblastoma culture models. *Neuro Oncol*. 2017;19(6):820–32.
  16. Chitnis GD, Verma MKS, Lamazouade J, Gonzalez-Andrades M, Yang K, Dergham A, Jones PA, Mead BE, Cruzat A, Tong Z, Martyn K, et al. A resistance-sensing mechanical injector for the precise delivery of liquids to target tissue. *Nat Biomed Eng*. 2019;3(8):621–31.
  17. Gonzalez LM, Moeser AJ, Blikslager AT. Porcine models of digestive disease: the future of large animal translational research. *Transl Res*. 2015;166(1):12–27.
  18. Bassols A, Costa C, Eckersall PD, Osada J, Sabria J, Tibau J. The pig as an animal model for human pathologies: a proteomics perspective. *Proteomics Clin Appl*. 2014;8(9–10):715–31.
  19. Wedel T, Roblick U, Gleiss J, Schiedeck T, Bruch HP, Kuhnel W, Krammer HJ. Organization of the enteric nervous system in the human colon demonstrated by wholemount immunohistochemistry with special reference to the submucous plexus. *Ann Anat*. 1999;181(4):327–37.
  20. Graham KD, Lopez SH, Sengupta R, Shenoy A, Schneider S, Wright CM, Feldman M, Furth E, Valdivieso F, Lemke A, Wilkins BJ, et al. Robust, 3-dimensional visualization of human colon enteric nervous system without tissue sectioning. *Gastroenterology*. 2020;158(8):2221–35.e5.
  21. Petto C, Gabel P, Pfannkuche H. Architecture and chemical coding of the inner and outer submucous plexus in the colon of piglets. *PLoS One*. 2015;10(7):e0133350.
  22. Mazzoni M, Caremoli F, Cabanillas L, de Los Santos J, Million M, Larauche M, Clavanzani P, De Giorgio R, Sternini C. Quantitative analysis of enteric neurons containing choline acetyltransferase and nitric oxide synthase immunoreactivities in the submucosal and myenteric plexuses of the porcine colon. *Cell Tissue Res*. 2021;383(2):645–54.
  23. Timmermans JP, Adriaensen D, Cornelissen W, Scheuermann DW. Structural organization and neuropeptide distribution in the mammalian enteric nervous system, with special attention to those components involved in mucosal reflexes. *Comp Biochem Physiol A Physiol*. 1997;118(2):331–40.
  24. Brown DR, Timmermans JP. Lessons from the porcine enteric nervous system. *Neurogastroenterol Motil*. 2004;16(Suppl 1):50–4.
  25. Li T, Morselli M, Su T, Million M, Larauche M, Pellegrini M, Tache Y, Yuan PQ. Comparative transcriptomics reveals highly conserved regional programs between porcine and human colonic enteric nervous system. *Commun Biol*. 2023;6(1):98.
  26. Sangild PT, Ney DM, Sigalet DL, Vegge A, Burrin D. Animal models of gastrointestinal and liver diseases. Animal models of infant short bowel syndrome: translational relevance and challenges. *Am J Physiol Gastrointest Liver Physiol*. 2014;307(12):G1147–68.
  27. Almond S, Lindley RM, Kenny SE, Connell MG, Edgar DH. Characterisation and transplantation of enteric nervous system progenitor cells. *Gut*. 2007;56(4):489–96.
  28. Hotta R, Stamp LA, Foong JP, McConnell SN, Bergner AJ, Anderson RB, Enomoto H, Newgreen DF, Obermayr F, Furness JB, Young HM. Transplanted progenitors generate functional enteric neurons in the postnatal colon. *J Clin Invest*. 2013;123(3):1182–91.
  29. Hotta R, Cheng LS, Graham HK, Pan W, Nagy N, Belkind-Gerson J, Goldstein AM. Isogenic enteric neural progenitor cells can replace missing neurons and glia in mice with Hirschsprung disease. *Neurogastroenterol Motil*. 2016;28(4):498–512.
  30. Stavely R, Bhave S, Ho WLN, Ahmed M, Pan W, Rahman AA, Ulloa J, Bousquet N, Omer M, Guyer R, Nagy N, et al. Enteric mesenchymal cells support the growth of postnatal enteric neural stem cells. *Stem Cells*. 2021;39(9):1236–52.
  31. Metzger M, Bareiss PM, Danker T, Wagner S, Hennenlotter J, Guenther E, Obermayr F, Stenzl A, Koenigsrainer A, Skutella T, Just L. Expansion and differentiation of neural progenitors derived from the human adult enteric nervous system. *Gastroenterology*. 2009;137(6):2063–73.e4.
  32. Cheng LS, Hotta R, Graham HK, Belkind-Gerson J, Nagy N, Goldstein AM. Postnatal human enteric neuronal progenitors can migrate, differentiate, and proliferate in embryonic and postnatal aganglionic gut environments. *Pediatr Res*. 2017;81(5):838–46.
  33. Micci MA, Kahrig KM, Simmons RS, Sarna SK, Espejo-Navarro MR, Pasricha PJ. Neural stem cell transplantation in the stomach rescues gastric function in neuronal nitric oxide synthase-deficient mice. *Gastroenterology*. 2005;129(6):1817–24.
  34. Olson JC. Immunosuppressive drugs and associated complications in abdominal organ transplantation. *Curr Opin Crit Care*. 2022;28(2):208–15.
  35. Toniutto P, Germani G, Ferrarese A, Bitetto D, Zanetto A, Fornasiere E, Fumolo E, Shalaby S, Burra P. An essential guide for managing post-liver transplant patients: what primary care physicians should know. *Am J Med*. 2022;135(2):157–66.
  36. Muraoka K, Shingo T, Yasuhara T, Kameda M, Yuan W, Hayase H, Matsui T, Miyoshi Y, Date I. The high integration and differentiation potential of autologous neural stem cell transplantation compared with allogeneic transplantation in adult rat hippocampus. *Exp Neurol*. 2006;199(2):311–27.
  37. Rollo BN, Zhang D, Stamp LA, Menhennott TR, Stathopoulos L, Denham M, Dottori M, King SK, Hutson JM, Newgreen DF. Enteric neural cells from Hirschsprung disease patients form ganglia in autologous aneuronal colon. *Cell Mol Gastroenterol Hepatol*. 2016;2(1):92–109.
  38. Thomas AL, Taylor JS, Huynh N, Dubrovsky G, Chadarevian JP, Chen A, Baker S, Dunn JCY. Autologous transplantation of skin-derived precursor cells in a porcine model. *J Pediatr Surg*. 2020;55(1):194–200.



39. Burns AJ, Le Douarin NM. Enteric nervous system development: analysis of the selective developmental potentialities of vagal and sacral neural crest cells using quail-chick chimeras. *Anat Rec*. 2001;262(1):16–28.
40. Nagy N, Goldstein AM. Endothelin-3 regulates neural crest cell proliferation and differentiation in the hindgut enteric nervous system. *Dev Biol*. 2006;293(1):203–17.
41. Mwizerwa O, Das P, Nagy N, Akbareian SE, Mably JD, Goldstein AM. Gdnf is mitogenic, neurotrophic, and chemoattractive to enteric neural crest cells in the embryonic colon. *Dev Dyn*. 2011;240(6):1402–11.
42. Fabbri C, Luigiano C, Lisotti A, Cennamo V, Virgilio C, Caletti G, Fusaroli P. Endoscopic ultrasound-guided treatments: are we getting evidence based—a systematic review. *World J Gastroenterol*. 2014;20(26):8424–48.
43. Chang KJ, Katz KD, Durbin TE, Erickson RA, Butler JA, Lin F, Wuerker RB. Endoscopic ultrasound-guided fine-needle aspiration. *Gastrointest Endosc*. 1994;40(6):694–9.
44. Giovannini M, Seitz JF, Monges G, Perrier H, Rabbia I. Fine-needle aspiration cytology guided by endoscopic ultrasonography: results in 141 patients. *Endoscopy*. 1995;27(2):171–7.
45. Bakker OJ, van Santvoort HC, van Brunschot S, Geskus RB, Besselink MG, Bollen TL, van Eijck CH, Fockens P, Hazebroek EJ, Nijmeijer RM, Poley JW, et al; Dutch Pancreatitis Study Group. Endoscopic transgastric vs surgical necrosectomy for infected necrotizing pancreatitis: a randomized trial. *JAMA*. 2012;307(10):1053–61.
46. Varadarajulu S, Bang JY, Sutton BS, Trevino JM, Christein JD, Wilcox CM. Equal efficacy of endoscopic and surgical cystogastrostomy for pancreatic pseudocyst drainage in a randomized trial. *Gastroenterology*. 2013;145(3):583–90.e1.
47. Artifon EL, Aparicio D, Paione JB, Lo SK, Bordini A, Rabello C, Otoch JP, Gupta K. Biliary drainage in patients with unresectable, malignant obstruction where ERCP fails: endoscopic ultrasonography-guided choledochoduodenostomy versus percutaneous drainage. *J Clin Gastroenterol*. 2012;46(9):768–74.
48. Chua T, Faigel DO. Endoscopic ultrasound-guided ablation of liver tumors. *Gastrointest Endosc Clin N Am*. 2019;29(2):369–79.
49. Levy MJ, Chak A; EUS 2008 Working Group. EUS 2008 Working Group document: evaluation of EUS-guided vascular therapy. *Gastrointest Endosc*. 2009;69(2 Suppl):S37–42.
50. Bick BL, Al-Haddad M, Liangpunsakul S, Ghabril MS, DeWitt JM. EUS-guided fine needle injection is superior to direct endoscopic injection of 2-octyl cyanoacrylate for the treatment of gastric variceal bleeding. *Surg Endosc*. 2019;33(6):1837–45.
51. Wyse JM, Carone M, Paquin SC, Usatii M, Sahai AV. Randomized, double-blind, controlled trial of early endoscopic ultrasound-guided celiac plexus neurolysis to prevent pain progression in patients with newly diagnosed, painful, inoperable pancreatic cancer. *J Clin Oncol*. 2011;29(26):3541–6.
52. Wiechowska-Kozłowska A, Boer K, Wojcicki M, Milkiewicz P. The efficacy and safety of endoscopic ultrasound-guided celiac plexus neurolysis for treatment of pain in patients with pancreatic cancer. *Gastroenterol Res Pract*. 2012;2012:503098.
53. Levy MJ, Alberts SR, Bamlet WR, Burch PA, Farnell MB, Gleeson FC, Haddock MG, Kendrick ML, Oberg AL, Petersen GM, Takahashi N, et al. EUS-guided fine-needle injection of gemcitabine for locally advanced and metastatic pancreatic cancer. *Gastrointest Endosc*. 2017;86(1):161–9.
54. Nakai Y, Chang KJ. Endoscopic ultrasound-guided antitumor agents. *Gastrointest Endosc Clin N Am*. 2012;22(2):315–24, x.
55. Martucciello G, Brizzolara A, Favre A, Lombardi L, Bocciardi R, Sanguineti M, Pini Prato A, Jasonni V. Neural crest neuroblasts can colonise aganglionic and ganglionic gut in vivo. *Eur J Pediatr Surg*. 2007;17(1):34–40.
56. Tsai YH, Murakami N, Garipey CE. Postnatal intestinal engraftment of prospectively selected enteric neural crest stem cells in a rat model of Hirschsprung disease. *Neurogastroenterol Motil*. 2011;23(4):362–9.
57. Navoly G, McCann CJ. Dynamic integration of enteric neural stem cells in ex vivo organotypic colon cultures. *Sci Rep*. 2021;11(1):15889.
58. Yasui Y, Yoshizaki H, Kuwahara T, Nishida S, Kohno M, Okajima H. Transplanted neural crest cells migrate toward Auerbach's plexus layer instead of the colon surface in recipient colon pretreated with collagenase and fibronectin. *Biochem Biophys Res Commun*. 2022;601:116–22.
59. Arnaud AP, Hascoet J, Berneau P, LeGouevic F, Georges J, Randuineau G, Formal M, Henno S, Boudry G. A piglet model of iatrogenic rectosigmoid hypoganglionosis reveals the impact of the enteric nervous system on gut barrier function and microbiota postnatal development. *J Pediatr Surg*. 2021;56(2):337–45.